SCIENTIFIC REPORTS

OPEN

SUBJECT AREAS:
CHEMICAL SYNTHESIS
SYNTHESIS AND PROCESSING
NANOSCALE BIOPHYSICS
DRUG DELIVERY

Received
18 April 2013

Accepted
2 December 2013

Published
6 January 2014

Correspondence and requests for materials should be addressed to X.G.Q. (xqu@ciac.ac.cn)

Non-Enzymatic-Browning-Reaction: A Versatile Route for Production of Nitrogen-Doped Carbon Dots with Tunable Multicolor Luminescent Display

Weili Wei, Can Xu, Li Wu, Jiasi Wang, Jinsong Ren & Xiaogang Qu

Laboratory of Chemical Biology, Division of Biological Inorganic Chemistry, State Key Laboratory of Rare Earth Resource Utilization, Changchun Institute of Applied Chemistry, Graduate School of the Chinese Academy of Sciences, Chinese Academy of Sciences Changchun, Jilin 130022, China.

The non-enzymatic browning, namely Maillard reaction is commonly invoked to account for abiotic chemical transformations of organic matter. Here we report a new reaction pathway via the Maillard reaction to systematically synthesize a series of nitrogen-doped carbon dots (C-dots) with superhigh quantum yield (QY) and tunable multicolor luminescent displayment. The starting materials are glucose and the serial amino acid analogues which allow systemically controlling luminescent and physicochemical properties of C-dots at will. Unexpectedly, the as-prepared C-dots possess bright photoluminescence with QY up to 69.1% which is almost the highest ever reported, favorable biocompatibility, excellent aqueous and nonaqueous dispersibility, ultrahigh photostability, and readily functionalization. We have demonstrated that they are particularly suitable for multicolor luminescent display and long-term and real-time cellular imaging. Furthermore, the methodology is readily scalable to large yield, and can provide sufficient amount of C-dots for practical demands.

Recently, carbon-based nanomaterials (CNMs) have received much attention because of their low toxicity, excellent solubility and stable photoluminescence (PL)[1–3]. Significant progress has been achieved on the utilization of CNMs as luminescent probes for bioimaging[4], optoelectronic devices[5], biosensors[6], and photocatalysis[7]. As a new comer in CNMs family, carbon dots (C-dots) which comprise discrete quasispherical nanoparticles with sizes below 10 nm[8], possess even more intriguing properties compared with other CNMs. Till now, a sheer variety of synthetic routes toward C-dots are available[9–11], and have made C-dot emitters as potential alternatives to the aforementioned PL CNMs in various applications[12–14]. Unfortunately, PL quantum yield (QY) of the previously reported C-dots is usually low (<15%)[8–11] with only a few exceptions that require laborious chromatographic further purification[15] or surface passivation[16]. In addition, although different emission color of C-dots could be observed by changing the excitation wavelength[17,18], preparation of C-dots with multi-emission colors under the same excitation wavelength remains a challenge, while this feature is crucial for multicolor patterning[19] and the related enticing applications[20–23], such as full-color displays[20], pixelated color structures[21] and sensor arrays[22]. Although an egg-derived C-dot with single blue-emitting color has evoked applications in these areas, simultaneous multi-color display in a single pattern was still failed even with the help of various organic dyes and toxic semiconductor quantum dots (QDs)[24]. Thus, a multicolor pattern with whole C-dots has never been achieved.

In parallel, it is common knowledge that even small modifications of the reaction parameters during synthesis can alter the properties of the resulting nanomaterials[25–27]. This is especially true in the synthesis of C-dots. In various cases, even the same starting materials could be led to C-dots with diverse properties due to the different reaction pathways[28–30]. For instance, by using activated carbon as the source, chemical oxidation[31] and ultrasonic treatment[32] resulted distinct blue and green emitting C-dots under UV excitation, respectively. Therefore, beyond starting materials, the reaction pathway plays crucial roles in the synthesis of C-dots with desired properties.

Herein, using nonenzymatic browning reaction[33,34], namely Maillard reaction, we report the first time a new reaction pathway for the synthesis of a series of nitrogen-doped C-dots with superhigh QYs, tunable multicolor luminescence. The Maillard reaction is commonly invoked to account for abiotic chemical transformations of

organic matter[35,36], and is ubiquitous in baking, toasting, and cooking of foods and *in vivo* in mammalian organisms[33–39]. In general, the Maillard reaction starts from the condensation between the aldehydes of reducing saccharides and the amino-containing proteins or amino acids, and ultimately leads to the formation of brown nitrogenous polymers, known as melanoidins[33–39]. More interestingly, it had been well proven by nuclear magnetic resonance technique, mass spectroscopy, and elemental analysis that different reaction precursors led to nitrogenous polymers varied in chemical composition and structures[34,38]. In view of this, different end products of the Maillard reaction could be used as building-blocks for further synthesis of nitrogen-doped C-dots with diverse electronic structure and chemical features of their cores and surface defects, respectively. Since the PL of C-dots depends on both the cores[15,29] and surface defects[8,29], the emission color would be easily tuned by using the basic biological building blocks (e.g., glucose and the natural amino acids containing versatile side chains) as starting materials. Whereas previously reported control of the subtle reaction parameters led to different emission color, the QYs of the resulting C-dots is fair and the method involved the requirement of high calcination temperature, inert reaction atmosphere, and special raw materials[28]. As far as we know, however, no attempt has been made by using Maillard reaction to systemically synthesize and tailor C-dots with tunable emission and physicochemical (e.g. zeta potential and lipophilicity) properties under uniform reaction parameters with a series of structurally defined analogues as starting materials. Furthermore, another obvious merit of these C-dots is the doping of N atoms, which usually enhances the emission QY[40,41].

Importantly, the present Maillard reaction-based approach is distinct to the previously reported methods that using organic acids, amines and saccharides alone or in combination as precursors[42–44]. In the present approach, starting materials were firstly transformed to nitrogenous polymers *via* the Maillard reaction pathway under specific conditions that is low moisture, high temperature, and moderate alkaline environment[33–39]. Nevertheless, extreme conditions such as concentrated sulfate and/or phosphate acids were commonly applied in previous methods for the direct carbonization of the starting materials[42–44]. As a consequence, the unique reaction pathway of the present method makes the PL and physicochemical properties of the C-dots different and superior. The QY of our C-dots can be up to 69.1%, which is almost the highest value that ever reported for the as-prepared C-dots without any further treatment. Due to the controllable luminescence, the C-dots have been demonstrated suitable for multicolor patterning and long-term and real-time medical diagnosis and cellular imaging.

Results

As shown in Figure 1, all the natural amino acids (Table S1), except Cys, Met, and Pro, were reacted systemically with glucose one by one to produce different C-dots through a simple microwave-assisted one-pot, two-step method. The two S-containing amino acids, Cys and Met were excluded due to the release of smelly by-products during the synthesis; and Pro was not used because it lacks of primary amine. The optimal reaction parameters were indicated in Figure 1, and the detailed synthesis procedures were provided in the Method Section. Here, microwave was essential due to its *in situ* and transient heating properties[45], which was extremely beneficial to the homogeneous formation of uniform nano-sized C-dots[46]. As a control, a hydrothermal reaction under similar conditions resulted in only micron-scale particles and this was in accordance with the previous reports[47]. The necessity of the Maillard reaction pathway was illustrated in the following sections.

All the 17 kinds of C-dots derived from corresponding amino acid and glucose were highly soluble in water and various organic solvents, such as methanol, dimethylformamide and dimethylsulfoxide; and part of them prepared with amino acids containing hydrophobic side chains, such as Leu and Ile, even showed amphiphilic properties allowing the dispersion in apolar solvents (e.g. tetrahydrofuran). Noticeably, these C-dots solutions exhibited a long-term (more than 6 months) homogeneous phase without any obvious precipitation at room temperature (Figure S1). The good dispersibility of the C-dots in both aqueous and nonaqueous solutions ensured their further applications.

The atomic force microscopy (AFM) and transmission electron microscopy (TEM) measurements were used for characterization of structure and morphology of all the C-dots. Figure 2 and Figure S2 showed typical TEM and AFM images of the Trp and glucose derived C-dots (Trp-C-dots), revealing the average height and diameter of 2.77 and 2.88 nm, respectively (Figure 2c and f). The results suggested that the Trp-C-dots should maintain a spherical shape. The high resolution TEM image (Figure 2e) further indicated the crystallinity of the Trp-C-dots, with a lattice parameter of *ca.* 0.23 nm, which was different to both the intra- and inter-plane lattice parameter (0.214 and 0.340–0.403 nm, respectively) of the reported C-dots derived from carbon sources without nitrogen[48]. The mismatch of lattice parameter could be attributed to the doping of nitrogen, and has also been found in other N-doped CNMs[41]. Similarly, the other C-dots all showed spherical shape with average sizes ranging from 2.2 to 5.1 nm (Figure S3–6, Table S2). Intriguingly, the size of the C-dots depended on the side-chain properties of the starting amino acids. Accordingly, the amino acids are categorized into four groups, which are neutral aliphatic, basic, aromatic and acidic amino acids (Table S1). The average sizes of the C-dots derived from acidic amino acids (e.g. Asp-C-dot, 4.93 nm) are apparently larger than those of other C-dots at a confidence level of 95%. This might be due to the acidic amino acids possess two carboxyl groups that can increase cross-linking between the amino acids and polyhydroxyl glucose. As well known, the carboxyl groups tend to forming esters with hydroxyls under conditions such as high temperature and low moisture[49]. In contrast, the basic amino acids (e.g. Arg) produced the smallest C-dots. This could be attributed to the relatively weak dissociation energies of N-containing bonds[50] and thus the products tend to be slipped into small pieces. The C-dots derived from aromatic and neutral aliphatic amino acids had moderate sizes.

Starting from Trp-C-dots, we explored the composition of the as-prepared C-dots with X-ray photoelectron spectroscopy (XPS) measurements. As seen in Figure 3a, the XPS survey of Trp-C-dots showed a predominant graphitic C 1 s peak at *ca.* 284 eV, an O 1 s peak at *ca.* 532 eV, and a pronounced N 1 s peak at *ca.* 400 eV. The O/C atomic ratio for Trp-C-dots (about 0.55) was much lower than that of the precursor glucose (1 : 1) due to the chemical transformation during the synthesis processes. The N/C atomic ratio was calculated to be 0.12, confirming the successful incorporation of N atoms into the C-dots by our two-step method. To illustrate the necessity of the step of Maillard reaction in Figure 1, the product obtained with the second step alone was poorly PL with N/C atomic ratio of only 0.02. The enlarged N 1 s peak of Trp-C-dots (Figure 3a) revealed the presence of secondary amine (399.5 eV, C-NH-C) and pyrrolic (400.8 eV, C=N-C) N atoms[41]. Apparently, the N species were different to that in the starting material Trp, further confirming the transformation and incorporation of N atoms in the C-dots. More chemical information of the C-dot was shown in the C 1 s spectrum (Figure 3c), where six peaks at 284.3 (sp^2 graphitic C), 284.9 (sp^3 graphitic C), 285.7 (C-N), 286.5 (C-O), 288.2 (C=O), 289.2 eV (COOH) were observed[41]. As shown in the Fourier transform infrared (FTIR) spectrum (Figure 3d), the vibration bands at 1396, 1276 and 3396, 1705 cm^{-1} demonstrated the presence of the respective aromatic amine (e.g. pyrrole ring), hydroxyl and carboxyl groups[40]. The structural information revealed by ^{13}C nuclear magnetic resonance (NMR) measurements were well consistent with the FTIR and XPS results (Figure S7). The ready presence of carboxyl groups allowed further linking of functional molecules through the

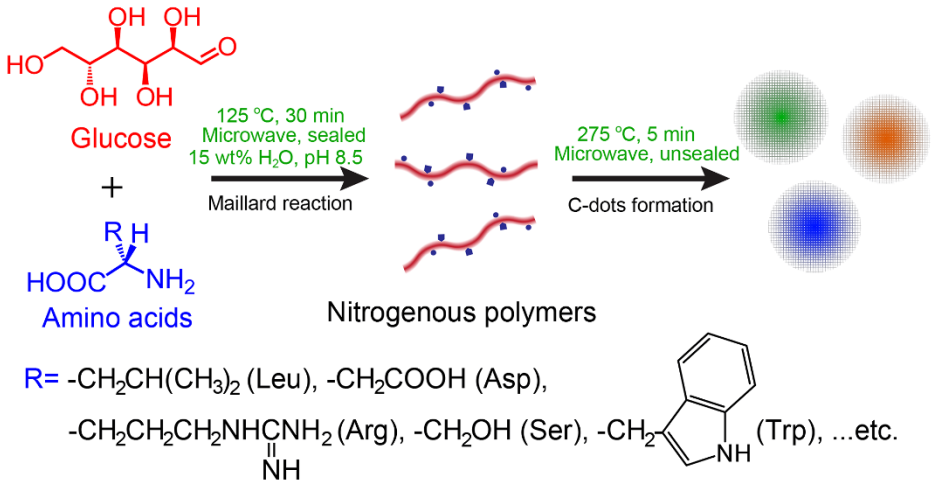

Figure 1 | **Schematic representation of the Maillard reaction directed a series of syntheses of nitrogen-doped C-dots with high PL QYs and tunable emission color.**

convenient *N*-hydroxysuccinimide (NHS) chemistry. Overall survey of the composition of the C-dots was carried out with XPS, FTIR and elemental analysis (Table S2). Similar to the size dependence, composition of the C-dots also showed a dependence on the side-chain properties of the starting amino acids. The N doping amount was highest for the basic amino acids derived C-dots (6.32–8.80 wt%), and the $-NH_2$ groups were abundant in them. As shown in Figure S8, the presence of $-NH_2$ in Arg-C-dots could be confirmed by the XPS peak at 401.6 eV (in $-NH_3^+$ form)[51]. This result could be attributed to the excess amount of amino groups in the raw materials. Akin to other PL CNMs (i.e. graphene and carbon nanotubes), the presence of sp^2 carbons in each kind of C-dots, especially in those derived from nonaromatic amino acids, was confirmed by both XPS and FTIR analysis (Figure S9–11). In addition, the C-dots were analyzed by gel permeation chromatography (GPC) with refractive index detection. For instance, only one main tailing peak with retention time of 20.88 min was found from the GPC chromatogram of Trp-C-dots (Figure S12). The molecular weight of the main peak was calibrated to be 9964 (Mw). According to TEM and FL investigation of different fractions, the minor peaks within 0–18.5 min were due to trace non-fluorescent and non-nanoparticle impurities which could be removed by further dialyzing; the main peak including its tailing parts was the C-dots with uniform diameter and PL properties. The GPC results indicated that all the above characterization techniques were measuring the C-dots.

In respect of the side-chain dependent size and composition, the physicochemical properties (e.g. lipophilicity and surface charge) were summarized in Table S2. Both the lipophilicity, in terms of octanol-water partition coefficients (Log*P*), and zeta potential of the C-dots spanned wide ranges from −3.12 (Asp-C-dot) to 0.23 (Leu-C-dot), and −45.1 mV (Asp-C-dot) to +37.2 mV (Arg-C-dot), respectively. As previously reported, surface charge and lipophilicity of nanoparticles had great effects on their cellular uptake, biodistribution, immune response and so on[52,53]. Therefore, using

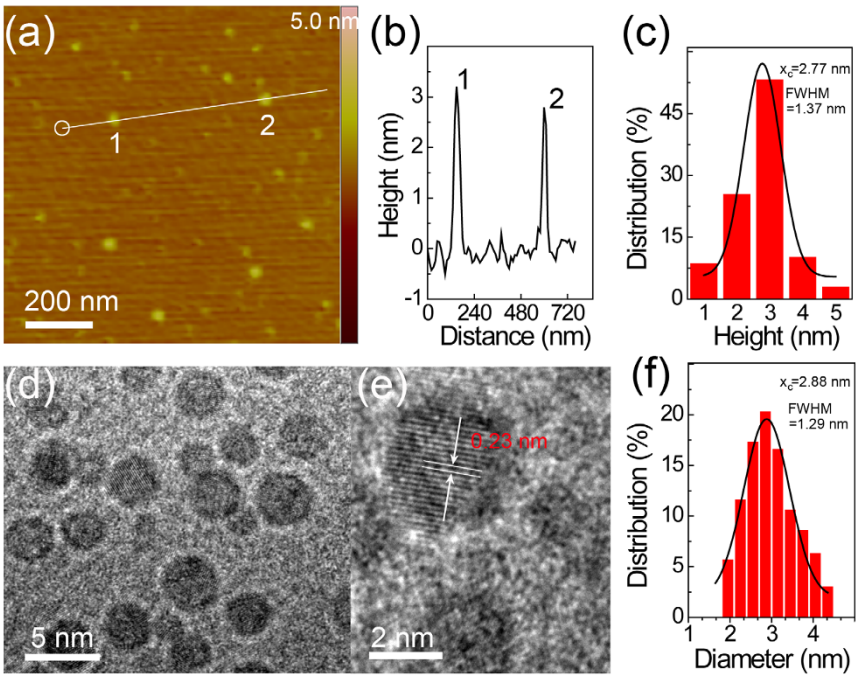

Figure 2 | (a) AFM image of Trp-C-dots on a mica substrate. (b) Height profile along the line in (a). (c) Height distribution of Trp-C-dots measured by AFM. (d, e) TEM images of the Trp-C-dots under different magnifications. (f) Diameter distribution of Trp-C-dots measured by TEM.

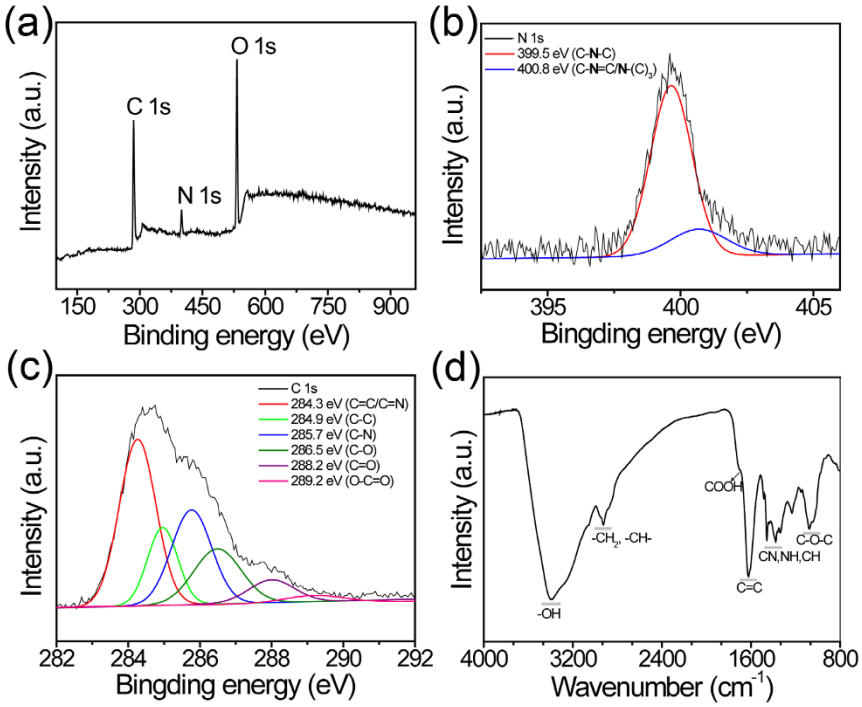

Figure 3 | (a) XPS spectrum of the as-prepared Trp-C-dot. (b, c) High-resolution N 1 s (b) and C 1 s (c) peaks of Trp-C-dot. (d) FTIR spectrum of Trp-C-dot.

Maillard reaction, we can prepare high QY nitrogen-doped C-dots with diverse physicochemical properties for versatile applications.

The PL properties of the C-dots were then characterized with emphasis. All the as-prepared C-dots could emit strong fluorescence with QY ranging from 30.2% to 69.1% (Table S2). The Trp-C-dot showed a very high QY up to 69.1%, and this was almost the highest value for the as-prepared C-dots without any further treatment. In addition to the high QYs, the C-dots showed different emission colors including blue, green, yellow, and orange. As summarized in Table S2, C-dots derived from basic and aromatic amino acids (e.g. Arg-C-dots and Trp-C-dots) showed blue emission; and those derived from neutral aliphatic (Leu-C-dots) and acidic (Asp-C-dots) emitted green and yellow (orange) color, respectively.

The blue, green and yellow emitting C-dots were carefully investigated with Trp-C-dot, Leu-C-dot, and Asp-C-dot as representatives. Figure 4a-c showed the 2D-PL topographical map of Trp-C-dot, Leu-C-dot, and Asp-C-dot, respectively. Obviously, they showed distinct excitation and emission properties. Under a wide range of excitation wavelengths used, the Trp-C-dots and Asp-C-dots just emitted blue light around 450 nm and yellow light around 560 nm, respectively, indicating that the emission of these two kinds of C-dots did not depend on the excitation wavelength. This was different from that usually observed excitation-dependent emission of C-dots prepared by other methods[9–14]. This phenomenon should be due to the Trp-C-dots and Asp-C-dots with narrow size distribution and uniform chemical features on their surfaces. The invariability of the emission wavelength is beneficial for applications in optoelectronics and bioimaging.

On the other hand, Leu-C-dot showed traditional excitation-dependent emission properties (Figure 4b). Although the maximum emission changes from *ca.* 450 to longer than 520 nm with increase of excitation wavelength, Leu-C-dot still showed green emission under a UV lamp (365 nm). Figure S13 showed different emission spectra under the same excitation wavelength (λ_{ex}=430 nm). The color coordinates of Trp-C-dot, Leu-C-dot, and Asp-C-dot were shown in Figure 4d. Noticeably, the coordinate of Trp-C-dot was (0.15, 0.14), indicating a deep-blue emission. Nowadays, solution-processable blue emitters are of unique technologic significance in the areas of display and lighting, because blue fluophors are usually low-molecular-weight molecules that typically require costly vacuum evaporation systems[54]. In view of this, the nano-scaled, highly solution processable, and strongly fluorescent Trp-C-dots should be a suitable candidate for those applications.

Further studies showed that the as-prepared C-dots had remarkable photostability. As shown in Figure S14, the fluorescence of the fluorescein isothiocyanate (FITC) was quickly quenched within 5 min under excitation due to severe photobleaching. The functional nanoprobe CdTe QDs[55] were more photostable, retaining >30% of the original PL intensity after 20-min excitation. In striking contrast, under *ca.* 60-min excitation, the PL intensity of all the C-dots we synthesized decreased slightly, preserving >90% of the initial intensity (Figure S14). The result indicated that PL of the C-dots was much more stable than the fluorescent FITC dye, CdTe QDs, and the previously reported dye-doped silica[56] or polymer nanoparticles[57] (Figure S14). The PL decay profiles of the C-dots were shown in Figure S15. The decay curves of both Trp-C-dot and Asp-C-dot fitted well to single-exponential with lifetimes (τ) of 22.6 and 8.62 ns, respectively. The single-exponential decay of Trp-C-dot or Asp-C-dot was consistent with the property of excitation-independent emission (Figure 4a, c), thus suggesting relatively uniform fluorescence radiative processes in the two kinds of C-dots[48]. However, the decay curve of Leu-C-dots fitted well to triple-exponential (Figure S15b) with a fast component (τ_1=0.69 ns) and two slow components (τ_2=5.00 ns and τ_3=10.96 ns), which was in accordance with the previously reports on lifetimes obtained from C-dots prepared by the electrochemical method[10]. The highly photostability and nanosecond lifetime suggested that these C-dots were most suitable for optoelectronic and biological applications. In addition, other optical properties of the C-dots including fluorescence upconversion (Figure S16) and electrochemiluminescence (Figure S17) were also observed primarily.

PL materials that can be used for multicolor luminescent patterning have drawn increasing interest in areas such as full-color displays, pixelated color structures and sensor arrays[20–23]. Prompted by the

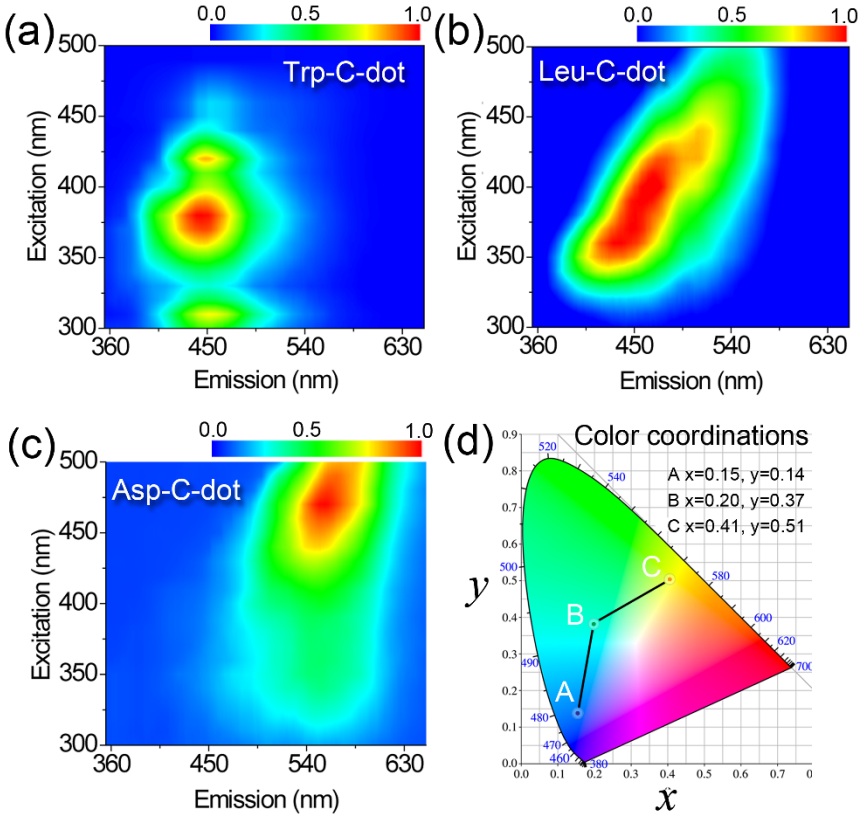

Figure 4 | 2D excitation-emission topographical maps of (a) Trp-C-dot, (b) Leu-C-dot, and (c) Asp-C-dot. The excitation and octave bands were filtered off during measurements. (d) Color coordinates of the 3 kinds of C-dots: A, Trp-C-dot; B, Leu-C-dot; and C, Asp-C-dot.

high QY, strong PL stability and unique emission, the Trp-C-dot, Leu-C-dot, and Asp-C-dot were used as blue, green, and yellow emitters, respectively. We first examined macroscopic patterning ability of the C-dots by imbedding them into the non-luminescent agarose gel. The tiny C-dots-embedded agarose gel slices (*ca.* 0.5 cm in diameter) could be used as pixels to smartly compose versatile patterns, such as a "Christmas tree" (Figure 5a). Long time stable, multicolor luminescence of such a pixilated pattern could be clearly observed under UV lamp (Figure 5b). In addition to the macroscopic patterning, the C-dots were also successfully applied to multicolor illuminating microscopic patterns in microchips (Figure S18). As shown in Figure 5d–e, the strips and letter pattern "CIAC" were clearly multicolor visualized with our C-dots, indicating that the C-dots could be used in multicolor luminescent patterning and related applications.

In addition to the excellent optical properties, the C-dots prepared from natural amino acids and glycoside as raw materials were non-cytotoxic under our experimental conditions (Figure S19). Due to good biocompatibility, the C-dots were further explored as biological fluorescent probes. For targeting Hela cells, the as-prepared C-dots were first conjugated with the folic acid *via* carboxylic acid groups on their surface. Folate receptors are over expressed on the surface of Hela cells, and thus folic acid-modified C-dots can specifically target cancer cells. Figure 6 showed the images of Hela cells treated with folic acid modified Trp-C-dot and Leu-C-dot for 4 hr incubation time, respectively. More significantly, the C-dots were particularly suitable for long-term and real-time cellular imaging due to their ultrahigh photostability in contrast to the bleaching FITC dye (Figure 6c, d).

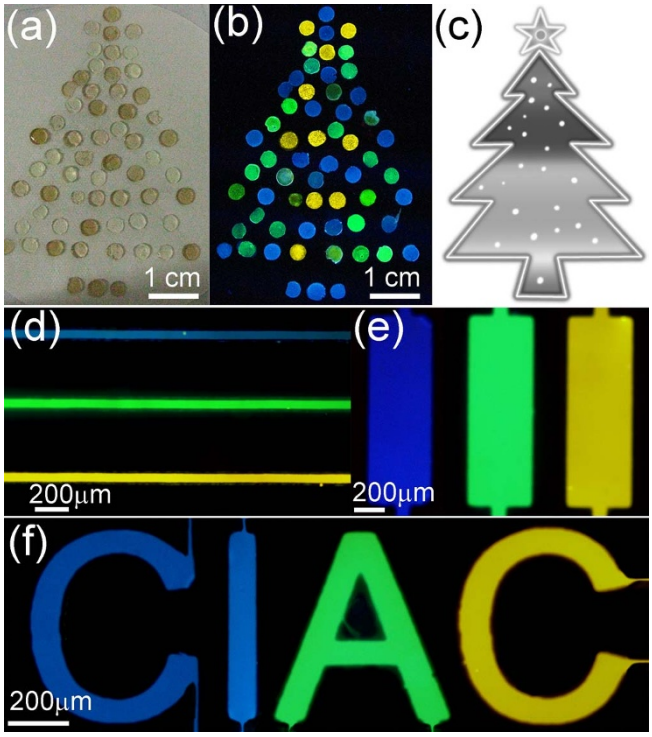

Figure 5 | Macroscopic photographs of the different C-dots-imbedded agarose gel slices patterned with a "Christmas tree" under (a) white light, and (b) UV lamp (350 nm) illumination. (c) The "Christmas tree" pattern. (d-e) Fluorescence microscope images of the different colored C-dots on PDMS chips with strips and "CIAC" pattern (λ_{ex}=430 nm).

Discussion

To the best of our knowledge, this is the first systemical tailoring of the emission and physicochemical properties of C-dots under

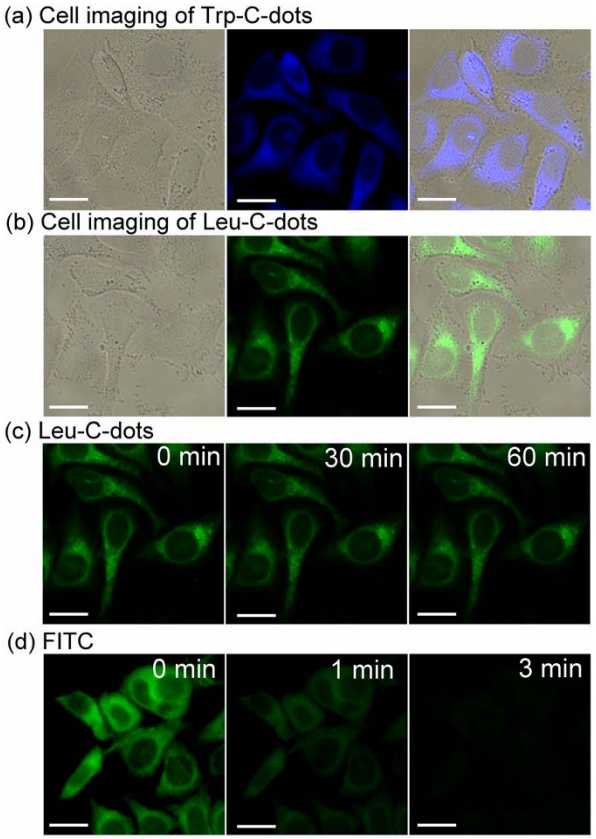

Figure 6 | Fluorescent images of Hela cell after incubation with (a) Trp-C-dot, and (b) Leu-C-dot for 4 h. (c, d) Stability comparison of fluorescence signals of Hela cells labeled by Leu-C-dot (c), and FITC (d). Scale bar=10 μm.

uniform reaction parameters with structurally defined analogues as starting materials. Different emission color should originate from C-dots of different size, shape, and composition-related factors, such as N-doping, content of sp^2 carbon and surface defects[8,41,58].

Firstly, among all the C-dots, the acidic amino acids derived C-dots had the largest size distribution, which could allow the existence of larger sp^2 conjugation of carbons in their cores. Both theoretical and experimental results have indicated that larger sp^2 conjugation of C atoms in another PL CNM, graphene quantum dots, can lead to emission at longer wavelength[1]. Similarly, the C-dots with larger sp^2 conjugation would emit longer wavelength showing yellow or orange color. Secondly, C-dots derived from basic amino acids had the smallest size distribution to emit at shorter wavelength, they emitted blue light. Although the size distributions of the neutral aliphatic and basic amino acids derived C-dots were similar, the former ones emitted green color. This should be due to the incorporation of higher content of N atoms in the basic amino acids-derived C-dots. As previously reported, doping of N atoms in CNMs usually induce PL blue shifted[41]. Finally, the unexpected intense blue emission of the aromatic amino acids-derived C-dots could attribute to the original sp^2 carbons in the starting materials. The original sp^2 carbons could be acted as building blocks to form C-dots with segregate small sp^2 carbon domains linked by oxygen-rich groups. This was structurally similar to the reduced-graphene oxide which also shows blue emission[54].

In summary, using the Maillard reaction, we have demonstrated a versatile route for scalable production of nitrogen-doped C-dots with superhigh QY and tunable multicolor luminescent display. The size and composition of the as-prepared C-dots vary with the side-chain structures of the starting amino acids, and the emission color and physicochemical properties (e.g. surface charge and lipophilicity) of the C-dots can be easily controlled accordingly. Significantly, the as-prepared C-dots possess strong PL (with QY up to 69.1%), favorable biocompatibility, excellent aqueous and nonaqueous dispersibility, ultrahigh photostability, and readily functionalization with surface carboxyl groups. Such resultant C-dots are particularly suitable for multicolor luminescent patterning and long-term and real-time cellular imaging. Therefore, the nonenzymatic browning reaction, Maillard reaction, which has been widely used in food industry and in biology, can also be a versatile approach to large-scale synthesis of C-dots for myriad applications in areas ranging from optoelectronic devices to medical diagnosis and biological imaging.

Methods

Synthesis of C-dots. The microwave synthesis was performed in the microwave system NOVA (Preekem, Shanghai, China). The system operates at 2450 MHz frequency and works at 0–500 W power. Each reaction was carried out in a sealed 50 mL glass vessel (with inner diameter of 2 cm) with less than 15 mL of raw materials. The average temperature of the vessel was obtained with a volume independent infrared sensor located inside the cavity of the microwave unit.

The general method for the synthesis of the C-dots was as follows: an equimolar mixture of glucose and an amino acid (5.6 mmol each) was loaded into a microwave reaction vessel, and water was added to an amount of 15 wt%. The mixture was sufficiently mixed via stirring and sonication. Before the vessel was sealed and placed into the microwave reactor, the acidity of the mixture was adjusted to pH 8.5 with 1 M NaOH solution. The vessel was placed in the microwave and heated at 125°C for 30 min. These reaction parameters were optimized to maximizing the Maillard reaction[33,34]. The nitrogenous polymers were efficiently produced with a yield of about 50% via Maillard reaction pathway during heat treatment. The molecular weight of the polymers was usually several kilodaltons as previously reported[38]. After this step, the vessel was cooled to room temperature, and unsealed in a desiccator for 20 min to absorb the vapors and volatile low molecular weight (<500 Da) products. The color of the first step treated-mixture was usually yellow or brown (related to the kind of amino acid that was used).

Subsequently, a second step was carried out for further formation of C-dots. The foregoing reaction vessel was placed into the microwave reactor and kept unsealed (to allowing evaporation of water) for a second short heating step (275°C, 5 min). Akin to many other approaches, the reaction vessel was kept unsealed in the second step for water evaporation which was beneficial to C-dots formation processes including dehydration, pyrolysis and surface passivation. The reaction conditions of this step were optimized via several parallel reactions. Upon completion of the microwave reaction, the reaction products were solubilized to 50 mL water, and then centrifugated (5000 rpm, 30 mim) to discard possible large and insoluble carbonized particles. The supernatants were collected and dialyzed (3000 kD tubing) for 24 h to obtain the final C-dots with a yield of ca. 20%–30%.

Characterization. Fluorescence measurements were carried out using a JASCO FP-6500 spectrofluorometer with the slit width for the excitation and emission of 5 nm. UV-vis filters of various wavelength were applied in the survey of the 2D topological excitation-emission maps of the C-dots. Ultraviolet-visible spectroscopy (UV-vis) measurements were recorded on a Jasco-V550 UV-Vis spectrophotometer. FTIR measurements were carried out with a BRUKER Vertex 70 FTIR spectrometer. The sample was prepared as pellets using spectroscopic grade KBr. AFM measurements were performed using a Nanoscope V multimode atomic force microscope (Veeco Instruments, USA) under ambient conditions, and samples were prepared by dropping the solution on mica. TEM experiments were performed using a Philips Tacnai G2 20 S-TWIN microscope operating at 200 kV. For visualization by TEM, samples were prepared by dropping a solution of production on a copper grid. XPS data were obtained with an ESCALab220i-XL electron spectrometer from VG Scientific using 300 W AlKα radiation. The base pressure was about $3\times10-9$ mbar. The binding energies were referenced to the C 1 s line at 284.8 eV from adventitious carbon. Curve fitting of the C 1 s and N 1 s spectra was performed using a Gaussian-Lorentzian peak shape. Fluorescence lifetime was measured with a Lecroy Wave Runner 6100 digital oscilloscope (1 GHz) using 355 and 405 nm laser (Continuum Sunlite OPO with pulse width = 4 ns) as excitation sources. Elemental analysis of the C-dots was carried out with Vanio-EL (Elementar Analysensysteme GmbH, Germany). Zeta potential measurements were performed on a Nano-ZS Zetzsozer ZEN3600 (Malvern Instruments Ltd., U.K.).

1. Peng, J. *et al.* Graphene quantum dots derived from carbon fibers. *Nano Lett.* **12**, 844–849 (2012).
2. Mochalin, V. N. & Gogotsi, Y. Wet chemistry route to hydrophobic blue fluorescent nanodiamond. *J. Am. Chem. Soc.* **131**, 4594–4595 (2009).
3. Chien, C.-T. *et al.* Tunable photoluminescence from graphene oxide. *Angew. Chem. Int. Ed.* **51**, 6662–6666 (2012).
4. Welsher, K. *et al.* A route to brightly fluorescent carbon nanotubes for near-infrared imaging in mice. *Nat. Nanotechnol.* **4**, 773–780 (2009).
5. Mueller, T. *et al.* Efficient narrow-band light emission from a single carbon nanotube p-n diode. *Nat. Nanotechnol.* **5**, 27–31 (2010).

6. Jung, J. H., Cheon, D. S., Liu, F., Lee, K. B. & Seo, T. S. A graphene oxide based immuno-biosensor for pathogen detection. *Angew. Chem. Int. Ed.* **49**, 5708–5711 (2010).
7. Zhuo, S., Shao, M. & Lee, S. T. Upconversion and downconversion fluorescent graphene quantum dots: ultrasonic preparation and photocatalysis. *ACS Nano* **6**, 1059–1064 (2012).
8. Baker, S. N. & Baker, G. A. Luminescent carbon nanodots: Emergent nanolights. *Angew. Chem. Int. Ed.* **49**, 6726–6744 (2010).
9. Liu, S. *et al.* Hydrothermal treatment of grass: A low-cost, green route to nitrogen-doped, carbon-rich, photoluminescent polymer nanodots as an effective fluorescent sensing platform for label-free detection of Cu(II) ions. *Adv. Mater.* **24**, 2037–2041 (2012).
10. Bao, L. *et al.* Electrochemical tuning of luminescent carbon nanodots: From preparation to luminescence mechanism. *Adv. Mater.* **23**, 5801–5806 (2011).
11. Liu, S. *et al.* Preparation of photoluminescent carbon nitride dots from CCl_4 and 1,2-ethylenediamine: a heat-treatment-based strategy. *J. Mater. Chem.* **21**, 11726–11729 (2011).
12. Wei, W., Xu, C., Ren, J., Xu, B. & Qu, X. Sensing metal ions with ion selectivity of a crown ether and fluorescence resonance energy transfer between carbon dots and grapheme. *Chem. Commun.* **48**, 1284–1286 (2012).
13. Zhu, A., Qu, Q., Shao, X., Kong, B. & Tian, Y. Carbon-dot-based dual-emission nanohybrid produces a ratiometric fluorescent sensor for in vivo imaging of cellular copper ions. *Angew. Chem. Int. Ed.* **51**, 7185–7189 (2012).
14. Liu, C. *et al.* Nano-carrier for gene delivery and bioimaging based on carbon dots with PEI-passivation enhanced fluorescence. *Biomaterials* **33**, 3604–3613 (2012).
15. Wang, X. *et al.* Bandgap-like strong fluorescence in functionalized carbon nanoparticles. *Angew. Chem. Int. Ed.* **49**, 5310–5314 (2010).
16. Sun, Y.-P. *et al.* Quantum-sized carbon dots for bright and colorful photoluminescence. *J. Am. Chem. Soc.* **128**, 7756–7757 (2006).
17. Liu, H., Ye, T. & Mao, C. Fluorescent carbon nanoparticles derived from candle soot. *Angew. Chem. Int. Ed.* **46**, 6473–6475 (2007).
18. Xu, Y. *et al.* Nitrogen-doped carbon dots: a facile and general preparation method, photoluminescence investigation, and imaging applications. *Chem. Eur. J.* **19**, 2276–2283 (2013).
19. Wang, Y., Tang, Z., Correa-Duarte, M. A., Liz-Marzan, L. M. & Kotov, N. A. Multicolor luminescence patterning by photoactivation of semiconductor nanoparticle films. *J. Am. Chem. Soc.* **125**, 2830–2831 (2003).
20. Wood, V. *et al.* Inkjet-printed quantum dot–polymer composites for full-color AC-driven displays. *Adv. Mater.* **21**, 2151–2155 (2009).
21. Li, Y., Urbas, A. & Li, Q. Reversible light-directed red, green, and blue reflection with thermal stability enabled by a self-organized helical superstructure. *J. Am. Chem. Soc.* **134**, 9573–9576 (2012).
22. Hu, C.-D. & Kerppola, T. K. Simultaneous visualization of multiple protein interactions in living cells using multicolor fluorescence complementation analysis. *Nat. Biotechnol.* **21**, 539–545 (2003).
23. Hu, W. *et al.* Multicolor emission on prepatterned substrates using a single dye species. *Adv. Mater.* **19**, 2119–2123 (2007).
24. Wang, J., Wang, C.-F. & Chen, S. Amphiphilic egg-derived carbon dots: rapid plasma fabrication, pyrolysis process, and multicolor printing patterns. *Angew. Chem. Int. Ed.* **51**, 9297–9301 (2012).
25. Liakakos, N. *et al.* The big impact of a small detail: cobalt nanocrystal polymorphism as a result of precursor addition rate during stock solution preparation. *J. Am. Chem. Soc.* **134**, 17922–17931 (2012).
26. Hu, J. *et al.* Linearly polarized emission from colloidal semiconductor quantum rods. *Science* **292**, 2060–2063 (2001).
27. Kwon, S. G. & Hyeon, T. Colloidal chemical synthesis and formation kinetics of uniformly sized nanocrystals of metals, oxides, and chalcogenides. *Acc. Chem. Res.* **41**, 1696–1709 (2008).
28. Guo, X., Wang, C.-F., Yu, Z.-Y., Chen, L. & Chen, S. Facile access to versatile fluorescent carbon dots toward light-emitting diodes. *Chem. Commun.* **48**, 2692–2694 (2012).
29. Krysmann, M. J., Kelarakis, A., Dallas, P. & Giannelis, E. P. Formation mechanism of carbogenic nanoparticles with dual photoluminescence emission. *J. Am. Chem. Soc.* **134**, 747–750 (2012).
30. Long, Y. M. *et al.* Shifting and non-shifting fluorescence emitted by carbon nanodots. *J. Mater. Chem.* **22**, 5917–5920 (2012).
31. Qiao, Z.-A. *et al.* Commercially activated carbon as the source for producing multicolor photoluminescent carbon dots by chemical oxidation. *Chem. Commun.* **46**, 8812–8814 (2010).
32. Li, H. *et al.* Synthesis of fluorescent carbon nanoparticles directly from active carbon via a one-step ultrasonic treatment. *Mater. Res. Bull.* **46**, 147–151 (2011).
33. Martins, S. I. F. S., Jongen,W. M. F. & Boekel, M. A. J. S. V. A review of Maillard reaction in food and implications to kinetic modeling. *Trends Food Sci. Technol.* **11**, 364–373 (2001).
34. Fang, X. & Schmidt-Rohr, K. Fate of the amino acid in glucose-glycine melanoidins investigated by solid-state nuclear magnetic resonance (NMR). *J. Agric. Food Chem.* **57**, 10701–10711 (2009).
35. Ikan, R. *et al.* Carbon-13 cross polarized magic-angle samples spinning nuclear magnetic resonance of melanoidins. *Org. Geochem.* **9**, 199–212 (1986).
36. Vandenbroucke, M. & Largeau, C. Kerogen origin, evolution and structure. *Org. Geochem.* **38**, 719–833 (2007).
37. Robert, F., Vera, F. A., Kervella, F., Davidek, T. & Blank, I. Elucidation of chemical pathways in the Maillard reaction by 17O-NMR spectroscopy. *Ann. NY Acad. Sci.* **1043**, 63–72 (2005).
38. Fay, L. B. & Brevard, H. Contribution of mass spectrometry to the study of the Maillard reaction in food. *Mass Spectrom. Rev.* **24**, 487–507 (2005).
39. Benson, L. M., Naylor, S. & Tomlinson, A. Investigation of Maillard reaction products using 15N isotope studies and analysis by electrospray ionization-mass spectrometry. *J. Food Chem.* **62**, 179–183 (1998).
40. Yang, Z. C., Li, X. & Wang, J. Intrinsically fluorescent nitrogen-containing carbon nanoparticles synthesized by a hydrothermal process. *Carbon* **49**, 5207–5212 (2011).
41. Li, Y. *et al.* Nitrogen-doped graphene quantum dots with oxygen-rich functional groups. *J. Am. Chem. Soc.* **134**, 15–18 (2011).
42. Jiang, J., He, Y., Li, S. & Cui, H. Amino acids as the source for producing carbon nanodots: microwave assisted one-step synthesis, intrinsic photoluminescence property and intense chemiluminescence enhancement. *Chem. Commun.* **48**, 9634–9636 (2012).
43. Zhai, X. *et al.* Highly luminescent carbon nanodots by microwave-assisted pyrolysis. *Chem. Commun.* **48**, 7955–7957 (2012).
44. Liu, C. *et al.* One-step synthesis of surface passivated carbon nanodots by microwave assisted pyrolysis for enhanced multicolor photoluminescence and bioimaging. *J. Mater. Chem.* **21**, 13163–13167 (2011).
45. Larthed, M., Moberg, C. & Hallberg, A. Microwave-accelerated homogeneous catalysis in organic chemistry. *Acc. Chem. Res.* **35**, 717–727 (2002).
46. Kim, S.-H., Lee, S. Y., Yi, G.-R., Pine, D. J. & Yang, S.-M. Microwave-assisted self-organization of colloidal particles in confining aqueous droplets. *J. Am. Chem. Soc.* **128**, 10897–10904 (2006).
47. Hu, B. *et al.* Engineering carbon materials from the hydrothermal carbonization process of biomass. *Adv. Mater.* **22**, 813–828 (2010).
48. Tang, L. *et al.* Deep ultraviolet photoluminescence of water-soluble self-passivated graphene quantum dots. *ACS Nano* **6**, 5102–5110 (2012).
49. Carey, F. A. & Sundberg, R. J. *Advanced Organic Chemistry*, Fourth Ed., Kluwer Academic Publishers, New York, 2002.
50. Blanksby, S. J. & Ellison, G. B. Bond dissociation energies of organic molecules. *Acc. Chem. Res.* **36**, 255–263 (2003).
51. Lim, I.-I. S. *et al.* Interparticle chiral recognition of enantiomers: A nanoparticle-based regulation strategy. *Anal. Chem.* **81**, 689–698 (2009).
52. Moyano, D. F. *et al.* Nanoparticle hydrophobicity dictates immune response. *J. Am. Chem. Soc.* **134**, 3965–3967 (2012).
53. Verma, A. & Stellacci, F. Effect of surface properties on nanoparticle-cell interactions. *Small* **6**, 12–21 (2010).
54. Eda, G. *et al.* Blue photoluminescence from chemically derived graphene oxide. *Adv. Mater.* **22**, 505–509 (2010).
55. Song, S. *et al.* Functional nanoprobes for ultrasensitive detection of biomolecules. *Chem. Soc. Rev.* **39**, 4234–4243 (2010).
56. Ow, H. *et al.* Bright and stable core-shell fluorescent silica nanoparticles. *Nano Lett.* **5**, 113–117 (2005).
57. Cong, L. *et al.* Uniform silica coated fluorescent nanoparticles: synthetic method, improved light stability and application to visualize lymph network tracer. *PLoS One* **5**, e13167 (2010).
58. Zhang, Z., Zhang, J., Chen, N. & Qu, L. Graphene quantum dots: an emerging material for energy-related applications and beyond. *Energy Environ. Sci.* **5**, 8869–8890 (2012).

Acknowledgments

This work was supported by 973 Project (2011CB936004, 2012CB720602), and NSFC (21210002, 91213302, 21303179).

Author contributions

J.R. and X.Q. designed research; W.W., C.X., L.W. and J.W. performed research; W.W., L.W. and J.W. analysed data; and W.W., J.R. and X.Q. wrote the paper.

Additional information

Supplementary information accompanies this paper at http://www.nature.com/scientificreports

Competing financial interests: The authors declare no competing financial interests.

How to cite this article: Wei, W.L. *et al.* Non-Enzymatic-Browning-Reaction: A Versatile Route for Production of Nitrogen-Doped Carbon Dots with Tunable Multicolor Luminescent Display. *Sci. Rep.* **4**, 3564; DOI:10.1038/srep03564 (2014).